J. Phys. IV France **10** (2000)
Pr9-51

Observation and modeling of dynamic recrystallization in high-strain, high-strain rate deformation of metals

M.A. Meyers, V.F. Nesterenko, J.C. LaSalvia*, Y.B. Xu** and Q. Xue

University of California, San Diego, Department of MAE, La Jolla, CA 92093, U.S.A.
** U.S. Army Research Laboratory, Aberdeen Proving Ground, Aberdeen, MD 21005, U.S.A.*
*** Institute of Metals Research, Chinese Academy of Sciences, Shenyang, China*

Abstract. The microstructural evolution inside shear bands was investigated experimentally and analytically. A fine recrystallized structure (grains with 0.05-0.3μm) is observed in Ti, Cu, 304 stainless steel, Al-Li, and Ta, and it is becoming clear that a recrystallization mechanism is operating. The fast deformation and short cooling times inhibit grain-boundary migration; it is shown that the time is not sufficient for migrational recrystallization. A rotational mechanism is proposed and presented in terms of dislocation energetics. This mechanism necessitates the stages of high dislocation generation and their organization into elongated cells. Upon continued deformation, the cells become sub-grains with significant misorientations. These elongated sub-grains break up into equiaxed grains with size of approximately 0.05-0.3 μm. It is shown that grain-boundary reorientation can operate within the time of the deformation process.

1. INTRODUCTION

It is impossible to resolve the details of microstructure evolution within shear bands by optical or scanning electron microscopy. Even transmission electron microscopy only reveals the recovered structure, that has undergone the plastic deformation and a complex thermomechanical history. Some of the earliest detailed observations by TEM were made by Stelly and Dormeval[1], Pak et al.[2], and Meyers and Pak [3] on shear bands produced in Ti-6Al-4V and commercial purity titanium. The electron diffraction patterns inside and outside of the shear band were radically different; outside the band, the characteristic pattern for a single crystalline orientation was clear. Inside the band, a ring-like pattern, produced by many crystallographic orientations, was apparent. The shear band consisted of equiaxed grains, with diameters of 0.05 - 0.2 μm. The dislocation density was relatively low. This remarkable feature led to the suggestion by Meyers and Pak [3] that the structure was due to dynamic recrystallization. Dynamic recrystallization in copper was first observed by Andrade et al.[5]; in Ti, by Pak et al.[2,3,7]; in tantalum, it was first observed by Meyers et al.[8], and Nesterenko et al.[9,10]; in Al-Li alloys, Chen and Vecchio[11]; in steels, Beatty et al.[12] and Meunier et al.[13] observed equiaxed grains even smaller(0.01 to 0.05 μm).The shiny, "transformed" appearance reported by many investigators in shear bands in steels is the result of a fine recrystallized structure with an associated dissolution of carbides, resulting in an increased resistance to etching. These features were in the past mistakingly identified as phase transformation products. Recent microscopic observations made within areas of intense plastic deformation in 304 stainless steel and an Al-Li alloy are shown in Figures 1(a) and (b), respectively. Since the thermo-mechanical history of the shear localization regions is rather complex, one asks the obvious questions:

a) *Do the observed recrystallization features occur during or after plastic deformation?*
b) What is the mechanism of recrystallization?

2. DEFORMATION AND COOLING TIMES

First, calculations will establish for titanium, copper, and tantalum, the plastic strains required to produce temperatures at which diffusional processes become important; this temperature is set as $0.4T_m$, where T_m is the melting temperature. This can be readily done by assuming adiabatic conditions for the deformation process and using a constitutive equation that incorporates strain hardening, strain-rate hardening, and thermal softening. The Johnson - Cook [14] equation, with a modified thermal softening term , $e^{-\lambda(T-Tr)}$ was

used for ease of integration. The temperature is (β is rate of conversion of deformation energy into heat, usually taken as 0.9):

$$dT = \left(\frac{\beta}{\rho C}\right)\sigma d\varepsilon \Rightarrow T = T_0 + \frac{1}{\lambda}\ln\left[e^{-\lambda(T_0-T_r)} + \left(\frac{\beta\lambda}{\rho C}\right)\left[1 + C_1 \ln\left(\frac{\dot{\varepsilon}}{\dot{\varepsilon}_0}\right)\right]\left[\sigma_0 + \left(\frac{k}{n+1}\right)\varepsilon^n\right]\varepsilon\right] \quad (1)$$

The other parameters have their usual meanings. The heat capacity is C and the density is ρ. The temperatures, normalized with respect to the melting temperature, are plotted in Figure 2(a) as a function of plastic strain for titanium, copper(shock hardened), and tantalum. The true strain(ε_t) required to reach the recrystallization range is material dependent. For titanium, the value is reached for ε_t = 1.2; for copper (shock-hardened to increase its flow stress) the strain is approximately 1.9; and for tantalum, the required strain is much higher, approximately 4.4. The strains generated in the hat-shaped specimen are sufficient to create these favorable thermal regimes for Cu, Ti and the Al-Li alloy. For Ta, the thick-walled cylinder method provides a better technique. The cooling times can be estimated from a computational heat-transfer analysis. The results are shown in Figure 2(b). Shear-band thicknesses were taken as 10, 200, and 100 μm for titanium, copper, and tantalum, respectively. These values are obtained from experimental measurements. If the recrystallized structure forms after deformation, a migrational mechanism is required, because of the absence of mechanical assistance. It is possible to estimate the size of the recrystallized grains assuming migrational recrystallization. To a first approximation, it is assumed that the following simple grain growth equation can be used[15]:

$$d \equiv k_0 \sum_{i=0}^{N}\left[\exp\left(-\frac{Q}{2RT(t_i)}\right)\right]\Delta t^{1/n} \quad (2)$$

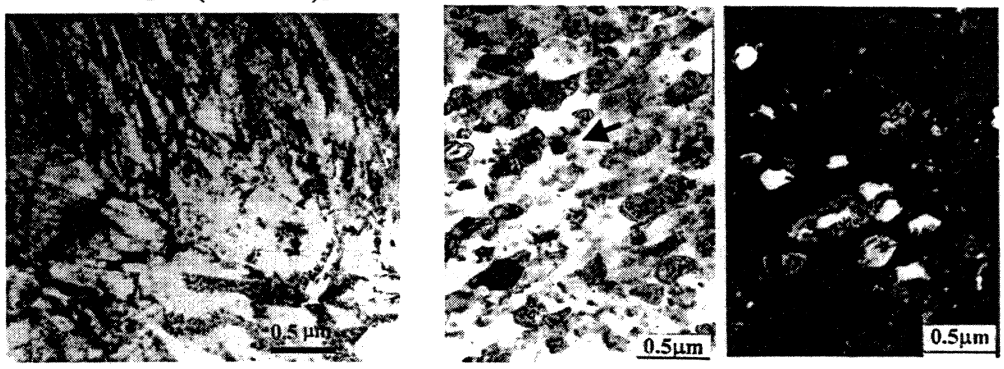

(a) (b)

Figure 1 TEM micrographs of microcrystalline structure within shear band (a)304 SS; (b) 8090Al-Li alloy (BF and DF).

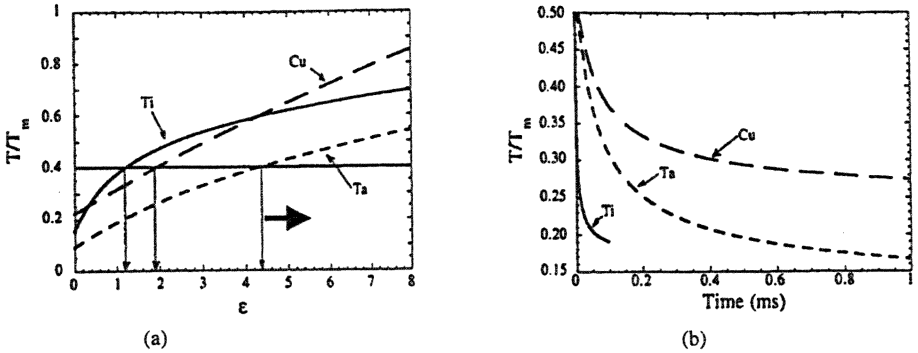

(a) (b)

Figure 2 (a) Normalized temperature as a function of plastic strain for titanium, copper, and tantalum

(b) Shear-band cooling curves for titanium, copper, and tantalum

where d is the instantaneous grain size , k_0 is a rate constant, Q is the activation energy for grain growth, Δt is the change in time t, and T is the absolute temperature. The activation energy for grain boundary migration can be taken as the activation energy for self-diffusion or for recrystallization. The pre-exponential factor k and exponent 1/n can be estimated from experimental results reported in the literature. A step-by-step derivation of the analytical derivations presented here will appear soon[16].The exponent n varies between 2 and 10 depending upon impurity content (e.g. n = 2 for ultra pure metals). The final grain size is obtained by numerically integrating Equation 2 during cooling. The values for Cu, Ta and Ti fluctuate around $2\sim9\times10^{-4}$ μm; this is clearly orders of magnitude smaller than the observed results and it is concluded that migrational recrystallization does not occur during cooling. It is also instructive to establish the deformation time. The deformation time t is simply given by the total strain divided by the strain-rate. These times are, respectively, for titanium, copper, and tantalum: $t=4 \times 10^{-5}$; 2.5×10^{-5}; and 10×10^{-5} s. Only a fraction of this deformation time occurs at a temperature sufficient to induce recrystallization. These times range, for the specimens analyzed, from 2 to 5×10^{-5} s. This time is lower by one order of magnitude than the cooling time(see Figure 2(b)). This would also exclude migrational recrystallization. *Thus a migrational mechanism alone cannot occur either in deformation or cooling and cannot account for the recrystallized structure.*

3. ROTATIONAL DYNAMIC RECRYSTALLIZATION

Derby[17] classifies dynamic recrystallization mechanisms into rotational and migrational types. Rotational recrystallization needs concurrent plastic deformation. It is well documented for geological materials such as quartz, halite, marble, and sodium nitrate. The observations in shear bands of copper, tantalum and titanium are suggestive of this mechanism. Figure 3 shows the primary features of the process by which rotational dynamic recrystallization is thought to occur. As can be seen from this figure, a homogeneous distribution of dislocations rearranges itself into elongated dislocation cells (i.e. dynamic recovery). As the deformation continues and as the misorientation increases, these cells become elongated subgrains. Eventually, the elongated subgrains break up into approximately equiaxed micrograins. These elongated subgrains are a characteristic feature of copper and titanium subjected to subrecrystallization strains. These elongated structures correspond to stage(c) in Figure 3 and are seen in many metals subjected to high strains, as reported by Gil Sevillano et al.[18], among others. The formation of these elongated sub-grains is analyzed below. This process of rotational recrystallization was modeled by Meyers et al.[19] using dislocation energetics. The strain energy for a random dislocation configuration (a in Figure 3) is given, per unit volume of material, by

$$E_1 = \rho_d \left(\frac{A\mu b^2}{4\pi} \right) \ln \left(\frac{\alpha}{2b\rho_d^{1/2}} \right) \tag{3}$$

where A is a constant depending upon the character of the dislocation, μ is the shear modulus, b is the magnitude of the Burgers vector, α is a constant which takes in account the core energy of the dislocation, ρ_d is the dislocation density. If the dislocations are arranged into cells, the energy is altered. A simple manner to represent the elongated cells is to assume that they are ellipsoidal. This corresponds to Configuration b in Figure 3. The cell walls can be modeled as tilt boundaries A dislocation density, ρ_d, can be assumed to be completely arranged in the cell walls. Equation 4 represents the energy if dislocations are arranged into cells:

$$E_2 = \rho_d \left(\frac{A\mu b^2}{4\pi} \right) \ln \left[\frac{e\alpha}{4\pi b} \left(\frac{S}{V} \right) \frac{1}{\rho_d} \right] \tag{4}$$

S and V are the surface and volume of the cell, respectively. Equations (3) and (4) give the total energy per unit volume due to the dislocations in Configurations a and b, respectively. For low dislocation densities, $E_1 > E_2$. The condition $E_1 = E_2$ gives the following expressions for the critical dislocation density ρ_d^* and misorientation angle θ^* at which Configuration b (Fig. 3) is of equal energy to Configuration a (assuming an aspect ratio, k, for the ellipsoids equal to infinity):

$$\rho_d^* = \left[\frac{3e}{8}\left(\frac{1}{W}\right)\right]^2 \qquad (5) \qquad\qquad \theta^* = \frac{3e^2}{8\pi}\left(\frac{b}{W}\right) \qquad (6)$$

Equations (5) and (6) are plotted in Figure 4 as a function of cell width for tantalum. The predicted misorientation angles for the observed cell widths are in excellent agreement with measured values. It is interesting to note that maximum energy difference between configurations a and b is given for an aspect ratio $k \to +\infty$. This is also consistent with observation that once the dislocation cells initially form, they are very long. These results are consistent with the TEM observations. A typical cell width varies between 0.1 and 0.3 μm, and cell formation occurs at a strain of approximately 1.8, with a temperature rise of 400K. This corresponds, approximately, to a dislocation density of 10^{10} cm^{-2}. The predictions of Figure 4 provide similar values for ρ^* and θ^* for dislocation densities in the range 10^{10}-10^{11} cm^{-2}.

The relaxation of the broken-down elongated sub-grains into an equiaxed micro-crystalline structure can occur by minor rotations of the grain boundaries lying along the original elongated boundaries, as shown in Figure 5. If each longitudinal grain boundary segment AB rotates to A'B' by an angle $\theta = 30°$, an equiaxed structure will be produced. This is illustrated in Figure 5(b). It will be shown how this can

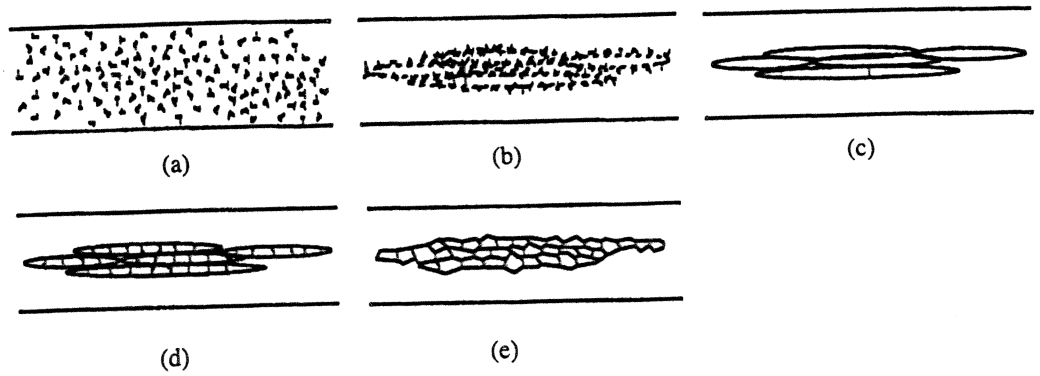

Figure 3 Schematic illustration of microstructural evolution during high-strain-rate deformation. (a) Randomly distributed dislocations; (b) Elongated dislocation cell formation (i.e. dynamic recovery); (c) Elongated subgrain formation; (d) Initial break-up of elongated subgrains; and (e) Recrystallized microstructure(from Nesterenko et al. [9]).

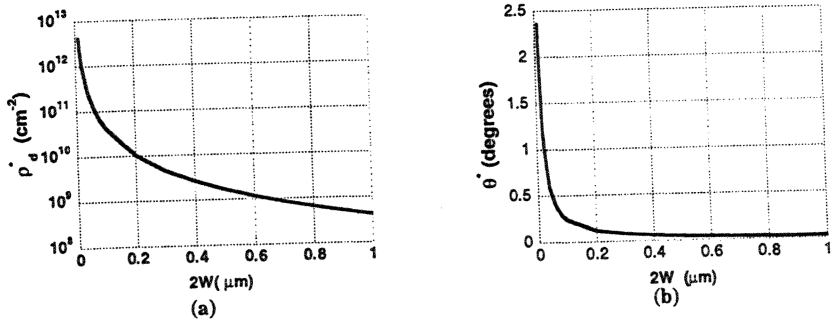

Figure 4 Critical dislocation density ρ^*_d (a) and resulting misorientation angle θ^* (b) as a function of cell width 2W.

be accomplished. The flux of atoms along the grain boundary can occur at rates that are orders of magnitude higher than in the bulk. The activation energy for grain boundary diffusion is approximately one half of that for lattice diffusion, and at $T/T_m = 0.5$, the ratio between grain boundary coefficient of diffusion, D_{GB} and lattice coefficient of diffusion, D_L varies between 10^7 and 10^8. These results are reported for FCC metals by Sutton and Balluffi[20] and Shewmon[21]. The activation energy for grain-boundary diffusion is approximately one half of that for lattice diffusion; hence, the difference increases as the temperature decreases. A general form of Fick's law, expressed in terms of a potential energy gradient, can be obtained[20,21]. The force $\vec{F}$, acting on a particle, is:

$$\vec{F} = \nabla V \tag{7}$$

where ∇V is the gradient of the potential energy field. The mean diffusion velocity $\vec{v}$ is the product of the mobility M by this force($\vec{v} = M\vec{F}$). The flux along a grain boundary with thickness δ and depth L_2 is equal to (the cross-sectional area is $L_2\delta$):

$$J = L_2 \delta C M F = \left(\frac{L_2 \delta D C_m}{kT} \right) F \tag{8}$$

where D is the diffusion coefficient. C_m, the concentration of the mobile species is expressed in terms of mass per unit volume.

The rotation of the boundaries is driven by the minimization of the interfacial energy. The force exerted by the grain boundaries is equal to:

$$F = \gamma \left(1 - 2\cos\frac{\theta_3}{2} \right) L_2 \tag{9}$$

This leads to:
$$\frac{d\theta}{dt} = \frac{4\cos^2\theta}{L_1^2 \rho} \frac{\delta D C_m}{kT} \gamma (1 - 2\sin\theta) L_2 \tag{10}$$

Integrating , we arrive at:

$$\frac{\tan\theta - \frac{2}{3}\cos\theta}{(1-2\sin\theta)} + \frac{4}{3\sqrt{3}} \ln \frac{\tan\frac{\theta}{2} - 2 - \sqrt{3}}{\tan\frac{\theta}{2} - 2 + \sqrt{3}} + \frac{2}{3} - \frac{4}{3\sqrt{3}} \ln \frac{2+\sqrt{3}}{2-\sqrt{3}} = \frac{4\delta D \gamma}{L_1 kT} t \tag{11}$$

The predictions of Equation 11 for copper are shown in Figure 6. In Figure 6(a) the temperature is varied from 0.35 to 0.5 T_m for a subgrain size of 0.3 μm; in Figure 6(b) the sub-grain size, L, is varied from 0.1 to 1 μm. The parameters used in Equation 11 are: γ=0.625 J/m^2[22]; δ(grain-boundary thickness)=0.5nm[21]; D_{GB}(grain-boundary diffusion coefficient)=$10^{-12.3}$-$10^{-15.5}$ m^2/s for T/T_m=0.5-0.35[22]. The rate of rotation decreases with increasing θ and asymptotically approaches 30° as $t \to \infty$. The calculations predict significant rotations of the boundary within the deformation time (~5 x 10^{-5} s or 0.05 ms) at temperatures of 0.45 and 0.5 T_m, for micrograin sizes of 0.1-0.3 μm. *Thus, the second stage of rotational recrystallization can also take place during plastic deformation.* This does not exclude the possibility of reorientation/accommodation of the grain boundaries during cooling.

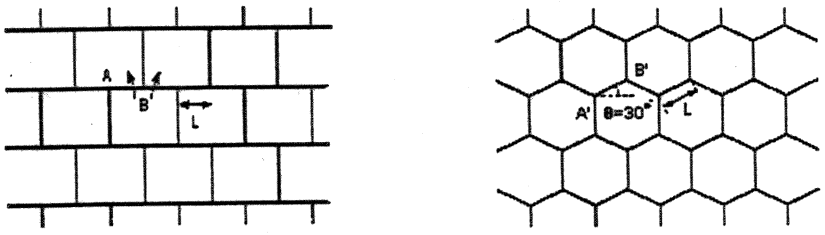

(a) (b)

Figure 5 Rotation of grain boundaries leading to equiaxed configuration: (a) broken down subgrains; (b) rotation of boundaries;

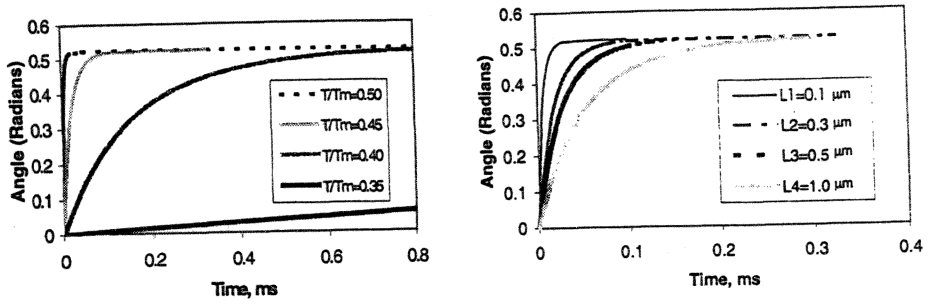

(a) (b)

Figure 6 Angle of rotation of micro-grain boundary AB as a function of time for (a) different temperatures and (b) different lengths(0.1, 0.3, 0.5, and 1 μm) at T/T_m=0.45.

4. CONCLUSIONS

Calculations reveal that the break-up of the elongated sub-grains and diffusive rotation of the grain boundaries can occur during the dynamic deformation process, leading to dynamic recrystallization in shear bands. This is direct support for the mechanism of rotational dynamic recrystallization postulated by Meyers and Pak[3] and Meyers et al. [7] for titanium, Andrade et al.[5,6] for copper, and Nesterenko et al.[9] for tantalum.

Acknowledgement: Research supported by U. S. Army Research Office MURI program.

REFERENCES

[1] Stelly, M. and Dormeval, R., in" Metallurgical Applications of Shock-Wave and High –Strain-Rate Phenomena " eds. L. E. Murr, K. P. Staudhammer, and M. A. Meyers, M. Dekker, 1986, p.607.
[2] Pak, H.–r., Wittman, C. L., and Meyers, M. A., ibid., p.749.
[3] Meyers, M.A. and Pak, H.-r., Acta Met., 34 (1986) 2493.
[4] Meyers, M.A., Meyer, L.W., Beatty, J., Andrade, U., Vecchio, K.S. and Chokshi, A.H., in *Shock-Wave and High-Strain-Rate Phenomena in Materials,* M. Dekker, New York, 1992, p 529.
[5] Andrade, U.R., Meyers, M.A., Vecchio, K.S. and Chokshi, A.H., Acta Metall.Mater., **42**(1994), 3183
[6] Meyers, M.A., Andrade, U., and Chokshi, A.H., Metall. Mat. Trans. A, **26A**, 1995, 2881.
[7] Meyers, M.A., Subhash, G., Kad, B.K., and Prasad, L., Mech. Mater., **17**(1994) 175.
[8] Meyers, M.A., Chen, Y.J., Marquis, F.D.S. and Kim, D.S., Metall. Mater. Trans., 26A (1995) 2493.
[9] Nesterenko, V.F., Meyers, M.A., LaSalvia, J. C., Bondar, M.P., Chen, Y.-J. and Lukyanov, Y.L., Mater. Sci. & Eng., **A229** (1997), 23.
[10] Chen, Y.-J., Meyers, M.A., and Nesterenko, V.F., Mater. Sci. & Eng., **A268**(1999) 70.
[11] Chen, R.W., and Vecchio, K. S., J. de Physique IV, **4**(1994) C8-459.
[12] Beatty, J.H., Meyer, L.W., Meyers, M.A., and Nemat-Nasser, S., in "*Shock-wave and High-Strain Rate Phenomena in Materials*", M. Dekker, NY, 1992, p.645.
[13] Meunier, Y., Roux, R., and Moureand, J., ibid., p.637
[14] Johnson, G.R. and Cook, W.H., Proc. 7th Int. Symp. Ballistics, ADPA, Netherlands, 1983.
[15] Reed-Hill, R.E. and Abhaschian, R., "*Physical Metallurgy Principles*", PWS Kent, Boston, MA, p.261.
[16] Meyers, M.A., Nesterenko, LaSalvia, V. F., J. C., and Xue, Q., Matls. Sci. and Eng., in press, 2000.
[17] Derby, B., Acta Metall., **39**(1991) 955.
[18] Sevillano, J. Gil, van Houtte, P., and Aernoudt, E., Progress in Matls. Sci., **25**(1981) 69.
[19] Meyers, M.A., LaSalvia, J.C., Nesterenko, V.F., Chen, Y.J., and Kad, B.K., in *"Recrystallization and Related Phenomena"*, ed. T.R. McNelley, Rex'96, Monterey, 1997, p.279.
[20] Sutton,A.P. and Balluffi,R.W., "*Interfaces in Crystalline Materials*", Clar. Press, Oxford, 1995, p.474
[21] Shewmon, P.G., "*Diffusion in Solids*", Second Ed., TMS-AIME, Warrendale, PA, 1989, p.31, p.200
[22] Murr, L.E., "*Interfacial Phenomena in Metals and Alloys*", Addison-Wesley, 1975, p.131.